Genomic Profiling of Pediatric ALK-Positive Anaplastic Large Cell Lymphoma: A Children's Cancer and Leukaemia Group Study

Catrin Youssif,[1] Jan Goldenbogen,[1] Rifat Hamoudi,[1] Joaquim Carreras,[1] Maria Viskaduraki,[2] Yu-xin Cui,[1] Chris M. Bacon,[3] G. A. Amos Burke,[4] and Suzanne D. Turner[1]*

[1]Division of Molecular Histopathology, Department of Pathology, University of Cambridge, Cambridge, UK
[2]Children's Cancer and Leukaemia Group, University of Leicester, Leicester, UK
[3]Northern Institute for Cancer Research, Newcastle University, UK
[4]Department of Paediatric Oncology, Addenbrooke's Hospital, Cambridge, UK

Anaplastic lymphoma kinase (ALK)-positive anaplastic large cell lymphoma (ALCL) is a T-cell malignancy in which ALK expression is a consequence of the t(2;5) or a variant translocation involving Chromosome 2. For the most part, this disease presents in the pediatric population and most, but not all, patients are successfully treated. Although the t(2;5) product nucleophosmin-ALK has been extensively studied for its transforming properties, very little is known regarding cooperative genetic mutations that may contribute to lymphomagenesis and may predict survival outcome, specifically in a purely pediatric population. We set out to determine the frequency and positions of genomic imbalances in this relatively rare disease. We collected biopsy material from 15 UK-resident children with ALK-expressing ALCL. We performed array comparative genomic hybridization at a resolution of 1 MB using DNA isolated from tumor tissue. Some of the more common genomic gains were confirmed by quantitative PCR. Regions of genomic gain were far more common than losses and were most often detected on chromosomes 1–4, 5–12, 14, and 17, with Chromosome 11 being the most frequent site of genomic imbalances. Patients with 14 or fewer imbalances had a lower overall 3-year survival (87.5–40%, $P = 0.14$) as did patients with gains in the regions of *DDB1* or *BIRC5*. A range of genomic imbalances exist in ALK-expressing ALCL of a pediatric origin, with a greater number associated with poorer overall survival.

INTRODUCTION

Anaplastic lymphoma kinase (ALK)-positive anaplastic large cell lymphoma (ALCL) is a T-cell malignancy characterized by the expression of the product of a chromosomal translocation involving the ALK gene on Chromosome 2 (Morris et al., 1994). The most common of these translocations is the t(2;5) generating the nucleophosmin (NPM)-ALK fusion protein, a hyperactive tyrosine kinase with transforming properties (Morris et al., 1994; Fujimoto et al., 1996; Turner and Alexander, 2006; Chiarle et al., 2008). NPM-ALK expression leads to the activation of a plethora of downstream signal transduction events including activation of the PI 3-Kinase, Ras-MAP Kinase, PLCγ, and Jak/STAT (Bai et al., 1998, 2000; Zamo et al., 2002; Zhang et al., 2002; Turner et al., 2007). These activities lead to increased survival and proliferation of the cells within which NPM-ALK is expressed and hence are consistent with oncogenesis. Indeed, transgenic mice expressing the NPM-ALK protein from a variety of hemopoietic-specific promoters develop lymphoma, albeit in a relatively long time frame (Chiarle et al., 2003; Turner et al., 2003, 2006; Turner and Alexander 2005).

The long latency to disease development in mouse models suggests that the acquisition of additional genetic aberrations is essential to the transforming process. However, ALCL is considered a relatively karyotypically stable disease suggesting that these additional events may be in the form of subtle genomic gains/losses or point mutations rather than gross chromosomal changes.

Additional Supporting Information may be found in the online version of this article.

Catrin Youssif and Jan Goldenbogen contributed equally to this work.

Supported by: The Leukaemia Research Fund (UK); The Kay Kendall Leukaemia Fund; Cancer Research UK; The Health Foundation/The Royal College of Pathologists/The Pathological Society of Great Britain and Ireland; The Leonardo Da Vinci Fund, EU Programme.

*Correspondence to: Suzanne D. Turner, Division of Molecular Histopathology, Department of Pathology, University of Cambridge, Lab Block Level 3, Box 231, Addenbrooke's Hospital, Cambridge CB20QQ, UK. E-mail: sdt36@cam.ac.uk

Received 11 May 2009; Accepted 15 July 2009

DOI 10.1002/gcc.20701

Published online 18 August 2009 in Wiley InterScience (www.interscience.wiley.com).

This led us to investigate what these secondary events might be. We have collected a database of 15 United Kingdom pediatric ALCL cases, all expressing NPM-ALK and many isolated from patients enrolled and treated on the EICNHL ALCL99 trial ($n = 13$) (Brugieres et al., 2009). We have performed array comparative genomic hybridization (aCGH) of 1-MB resolution to identify consistent regional genetic gains and losses.

MATERIALS AND METHODS

Patient Material

Fresh frozen (17 samples from 14 patients) or formalin-fixed paraffin embedded (FFPE) sections (one patient) were obtained from the Children's Cancer and Leukemia Group under study number 2006BS10 with approval from the appropriate research ethics committee (06/MRE04/90). Many of the cases are redundant archival biopsy specimens from the EICNHL ALCL99 clinical trial ($n = 13 + 3$ relapse samples) and all cases were reviewed histopathologically prior to DNA extraction. The phenotype of the tumors was assessed in CCLG member centers with pathological review within the United Kingdom. In brief, immunohistochemical analysis for T-cell markers (CD3, CD4, CD8, and CD30) and PCR for the presence of rearrangements of the T-cell receptor enabled the classification of cases into either a T- or null cell phenotype. ALK status was assessed by immunohistochemistry using ALK-specific antibodies. Follow-up clinical data were only available on the 13 trial cases and hence only these have been taken into consideration for analysis of survival. These data are reflected in Table 1 and Supporting Information Table 2.

DNA Extraction

Prior to DNA extraction, histopathological review of H&E stained sections was performed. Only tissues containing greater than 70% tumor cells were used for DNA extraction and additional experiments. Tumor content was determined by morphology by experienced pathologists (CMB and JC). In all cases our tissue sections contained greater than 70% tumor cells.

Sections were prepared for DNA extraction: Frozen tissue sections were dipped in distilled water and dried at room temperature for ~1 hr. FFPE samples were first incubated in an oven (56°C) overnight, deparaffinised, and rehydrated by immersion in xylene (twice for 10 min), 100% ethanol (twice for 5 min), 95% ethanol and 70% ethanol. Sections were then thoroughly washed in distilled water and left to dry at room temperature for ~1 hr. The prepared FFPE and frozen tissues were scraped with a surgical blade into 1.5-ml microcentrifuge tubes.

DNA extraction from ALCL and control tonsil samples was performed using a DNA Micro Kit (Qiagen, Hilden, Germany), according to the manufacturer's protocol, and eluted into 30-µl double distilled water. The DNA concentration of the extracted samples was measured using a fluorescent DNA quantification kit (Bio-Rad, CA) and a NanoDrop spectrophotometer (NanoDrop Technologies, Wilmington, USA).

The quality of each DNA sample was assessed by PCR amplification of variably sized DNA fragments using four different primer pairs as described in van Dongen et al. (2003). Further details of the quality criterion for inclusion in the study are detailed in the Supporting Information. All of our samples passed quality control and were included in the study.

Array Comparative Genomic Hybridization

DNA labeling reactions were performed using the Bioprime labeling kit according to manufacturer's instructions (Invitrogen, Carlsbad, CA). The Cy3 or Cy5 labeled dCTP was purchased from GE Healthcare, Chalfont St. Giles, United Kingdom. Cy5 was used for labeling the patient tumor DNA and Cy3 for the reference DNA (pooled DNA from the blood of 20 healthy men or women).

Following labeling, excess nucleotides were removed from the reaction using Micro-spin G50 columns (Pharmacia Amersham, Little Chalfont, United Kingdom). The success and efficiency of the labeling reaction was assessed by monitoring fluorescence intensity using a NanoDrop spectrophotometer.

We used a 1-Mb resolution genomic array containing 3,038 bacterial artificial chromosome (BAC) clones in duplicate produced at the microarray facility of the Department of Pathology, University of Cambridge (McCabe et al., 2006). Arrays were prehybridized for 2 hr at 37°C followed by hybridization for two nights at 37°C. The prehybridization buffer consisted of 40 µl of 10 mg ml^{-1} herring sperm DNA, 80 µl Human Cot1 DNA (Invitrogen), 20 µl distilled water, 18 µl 3 M NaAc pH 5.2, and 450 µl 100% ethanol. The hybridization buffer consisted of the Cy5

Genes, Chromosomes & Cancer DOI 10.1002/gcc

TABLE 1. Genomic Imbalances Detected by aCGH in Each Case Studied

Case	Outcome and follow-up time	Gains	Losses
4/59	Alive/Rx1/CR; 8.7 yrs	1p36.31-33, 1q32.1-32.2, 4p16.1-16.3, 7p11.2, 7p21.1-22.3, 7q11.23, 7q22.1-22.3, 7q36.1-3, 11p15.1-15.5, 11q12.2-11q13.3, 11q23.3-24.3, 16p13.1-3, 16q24.2-24.3, 18q23	
4/268	Dead/Rx1; 0.7 yrs	7p22.1-22.3, 7q36.1-3, 8q24.21-25.3, 9q34.13-34.3, 11p11.2-15.5, 11q12.2-23.3, 14q32.32-33, 14p15.3, 16p13.1-3, 16q24.3, 17q21.32, 20q13.33.	
4/303	Relapse of 4/268	1q21.1-32.1, 2q36.3-37.3, 2p25.1-3, 3p14.3-25.3, 3q21.3-29, 4p16.3, 5q31.3-35.3, 6p21.1-25.3, 6q21-37.1, 7p11.2-36.2, 7q22.1-36.3, 8q24.2-25.3, 10p14, 10q22.3, 11p15.5, 11q12.2-11q23.3, 12q13.11-24.3, 13q34, 14q11.2-36.3, 17p11.2-13.3, 17q21.31-32, 18q23.	11q13.4, 3p21.1, 9q13.4.
4/502	Alive/Rx2; 6.8 yrs	14q13.3.	12p11.22
4/503	1st relapse of 4/502	8p23.3-25.3.	3p12.2
4/534	2nd relapse of 4/502	5q31.1-35.3, 9q34.2-34.3, 9q13.3, 11q12.2-11q15.5, 11q23.3-24.3, 11p15.5, 14q24.3-32.12, 17q21.32, 20q13.3.	
4/454	Dead; 5.6 yrs	1p36.32, 1q21.1-32.1, 1q42.13-44, 2q13, 2q36.3-37.3, 2p11.2, 2p25.1-3, 3p25.1-3, 3q21.3, 4p16.3, 5q23.3-35.3, 6p21.1-25.3, 7p21.1-22.3, 7q22.1, 7q36.1-3, 8p11.2, 8p21.3-24.3, 8q23.1-25.3, 9q33.3-34.3, 9p11.2-13.2, 9p24.3, 10q11.21, 10q22.3-26.3, 11p15.5, 11q12.2-11q13.4, 11q23.3-24.3, 12q13.11-13.3, 12q24.3, 13q12.1-34, 14q24.3-32.33, 14p15.3, 16p11.2, 16p13.1-3, 16q23.2-24.3, 17p11.2-32.2, 17q21.2-25.3, 18p11.21.2, 18q23.	8p22, 3p21.1.
5/182	Alive/Rx1; 1.5 yrs	1p36.12, 1q21.1-32.1, 2q13, 2q24.3-25.3, 2q37.1-3, 2p11.2, 2p25.1-3, 4p16.3, 5q31.1-35.3, 6p21.1-25.3, 7p21.1-22.3, 7q22.1, 7q36.1-3, 8p11.2-24.3, 8q24.3-25.3, 9q34.13-34.3, 10q11.2-24.1, 10p15.1-3, 11p15.5, 11q12.2-11q13.4, 14q32, 12-32, 14p14.3, 16p13.1-3, 16q12.1-24.3, 17p11.2-13.3, 17q21.2-25.3, 18q23.	22q21.21
5/293	Alive/Rx1; 4.4 yrs	2q37.3, 2p25.1-3, 6p25.3, 7p22.3, 7q22.1, 7q36.1-3, 9q34.13-34.3, 11q12.2-13.4, 11q24.3, 11p15.5, 12q13.11-13.13, 14p15.3, 17q25.3, 18q23.	
5/306	Dead/Rx1; 4.5 yrs	1q21.1-32.1, 2q37.3, 2p24.3-25.1-3, 4p16.3, 5q31.1-35.3, 6q25.3, 6p21.1-25.3, 7p11.2, 7p21.1-22.3, 7q22.1, 7q32.236.1-3, 9q34, 10q22.3, 11p15.5, 11q12.2-11q13.4, 11q23.3-24.3, 12q13.11-13.3, 12q24.3, 14q32.12-32, 16p13.1-13.3, 16q24.3.	
5/381	Alive/CR; 4.9 yrs	3p21.32-22.1, 14q13.3.	12p11.22, 22q21.21
7/136	Dead; 1.4 yrs	1p34.3, 8p23.1, 9p13.2.	8p22, 12p11.22, 22q21.21
12/275	Alive/Rx3/CR; 3.8 yrs	2q37.1-3, 2p25.1-3, 5q23.3-35.3, 6p21.1-25.3, 6q25.3, 7q36.1-3, 9q34.13-34.2, 9p11.2-13.1, 10q22.3-26.3, 11p11.2-15.5, 11q12.2-11q13.4, 11q23.3-24.3, 12q13.11-13.3, 12q24.3, 14q24.3-32.33, 16p13.1-3, 16q24,3, 17p11.2-13.3, 17q21.31-25.3.	
14/125	Dead/Rx1; 0.7 yrs	2q34-37.3, 6p21.1-25.3, 6q27, 7q36.1-3, 9q34.13-34.3, 10q22.3, 11p15.5, 11q12.2-11q23.3 12q12.11-24.3, 13q12.13-34, 14q24.3-34.33, 14p15.3, 15q15.1-26.1, 16p13.1-3, 16q24.3, 17p11.2, 17q21.2-25.3.	3p12.2-21.2, 15q24.1-26.1
14/211	Alive/Rx2; 1.5 yrs	1p36.32, 10q22.3, 11q13.4	
18/40	Alive/CR; 0.2 yrs	1p36.11-32, 4p16.1-3, 7p21.1-36.2, 7q11.20-23, 7q22.1, 7q36.1-3, 9q34.2-3, 11p15.5, 11q12.2-11q13.2.	
F-1	Unknown	1q32.1, 2q36.3-37.3, 2p25.1-3, 6p21.3, 7p21.1-22.3, 7q22.1, 7q36.1-3, 8q24.3-25.3, 9p24.3, 9q34.13-34.3, 10q22.3-26.3, 11q12.2-13.1, 11p15.5, 16p13.1-3, 16q24.3, 17p11.2-13.3, 17q21.2-25.3, 18q23, 21q22.1-3.	
S-04-9794	Unknown	1p36.12-32, 1q21.1-44, 2q36.3-37.3, 2p25.1-3, 4p16.3, 5q31.1-35.3, 6p21.1-3, 7p13-22.3, 7q22.1, 7q32.2-36.1-3, 10q22.3, 11p15.5, 11q12.2-11q13.4, 11q23.3-24.3, 14q24.1-32.33, 15q15.1-26.1, 16p11.2-13.3, 16q24.3, 17p11.2-13.3, 17q21.2-25.3, 21q22.1.	

CR = complete remission at time of follow-up, R = relapse within follow-up period.

TABLE 2. Primers Used for Q-PCR Confirmation of Copy Number Gain

Gene	Primer name	Sequence	Product size (bp)
Ribosomal 18S RNA	18SRNAfwd	forward: 5′- tgactcaacacgggaaacc -3′	130
	18SRNArev	reverse: 5′ – tcgctccaccaactaagaac -3′	
DNA damage-binding protein 1	DDB1fwd	forward: 5′ - atgacgatggcagcggtatg – 3′	167
	DDB1rev	reverse: 5′– caagaagacgatggtggagagg – 3′	
v-Ha-ras Harvey rat sarcoma viral oncogene homolog	HRASfwd	forward: 5′ - gtcagcagcctcccttgtg – 3′	98
	HRASrev	reverse: 5′ – tccttccttcctcctccttcc – 3′	
Homeobox B1 protein	HOXB1fwd	forward: 5′ – ctgtccagccctgcgtttc – 3′	174
	HOXB1rev	reverse: 5′ – gcctccgtctccttctgattg – 3′	
Baculoviral IAP repeat-containing protein 5	BIRC5fwd	forward: 5′ - ggtcatctcggctgttcctg – 3′	144
	BIRC5rev	reverse: 5′ – cctcactgcggctgtctggg – 3′	

labeled tumor DNA and the Cy3 labeled reference DNA together with 20 μl of 10 mg ml^{-1} herring sperm DNA, 45 μl human Cot1 DNA (Invitrogen), 18 μl 3 M NaAc pH 5.2, and 450 μl cold 100% ethanol.

Following hybridization, the array slides were washed with shaking at 150 rpm in PBS/0.05% Tween 20 for 5 min, PBS/0.05% Tween 20 for 15 min, 0.1 × SSC for 30 min, twice in PBS/0.05% Tween 20 for 15 min, three times in 1 × PBS for 5 min. To validate our data, DNA isolated from reactive tonsil samples were labeled and applied to arrays and a representative example is shown in the Supporting Information Figure 2.

Data Analysis

Slides were scanned using an Axon 4100A scanner and images quantified using GenePix Pro 6.0 software (Axon instruments, Burlingame, CA). Primary data analysis and normalization were carried out using Microsoft Excel (Johnson et al., 2006; McCabe et al., 2006). The average of the duplicate spotted BACs on the microarray slides was calculated and results were analyzed using plots of $\log_2$-transformed normalized Cy5:Cy3 intensity ratios against clone position.

Major aberrations were easily detected by visual inspection of the aCGH plot, by which gains/losses of contiguous BACs were easily identified. Because of the high quality of our DNA from frozen tissue and the 1 FFPE case and the success of labeling reactions, background noise was minimal (see Supporting Information Fig. 3). However, to facilitate the detection of changes in a systematic manner, an in-house statistical smoothing approach based on Hidden Markov Models was applied (Chanudet et al., 2009). Further details are provided in the Supporting Information.

Genes of interest within recurrent amplified or deleted regions were examined with the aid of the Ensembl genome browser (http://www.ensembl.org/Homo_sapiens).

Quantitative PCR

Primers were designed to detect copy number changes of four specific genes, namely DNA damage-binding protein 1 (*DDB1*), Harvey rat sarcoma viral oncogene homologue (*HRAS*), *BIRC5*, and Homeobox B1 protein (*HOXB1*) (Table 2). Q-PCR was carried out using DNA isolated as detailed above and an iCycler iQ system (Bio-Rad, Hemel Hempstead, United Kingdom) with Absolute Blue Q-PCR SYBR Green. Human 18 s rRNA was used as an internal control. The conditions for real-time PCR were systematically optimized prior to data collection. Briefly, the specificity of the PCR products for each primer set was confirmed by melt-curve analysis and by electrophoresis on 6% polyacrylamide gels. Following optimization of reaction conditions, Q-PCR was performed in a 25-μl reaction volume containing 12.5 μl Absolute Blue Q-PCR SYBR Green Mix (Fisher Scientific, Loughborough, United Kingdom), 50 ng of template DNA, and 70 nmol l^{-1} each of both sense and antisense primers. All samples were amplified in triplicate in a 96-well PCR plates by 40 cycles at 95°C for 15 sec, 60°C for 30 sec, with one preceding cycle of enzyme activation at 95°C for 15 min. Q-PCR of the internal control was run in parallel for each sample. Melt-curve analysis was performed immediately following amplification for each case and only samples that showed specific amplification were included in the data. The CT values were obtained for each sample and the ΔCT value was calculated by subtracting the CT value of 18 s rRNA from the experimentally obtained values of the targets. Further, ΔΔCT values were calculated by subtracting the obtained ΔCT values of those obtained from control tonsil tissue.

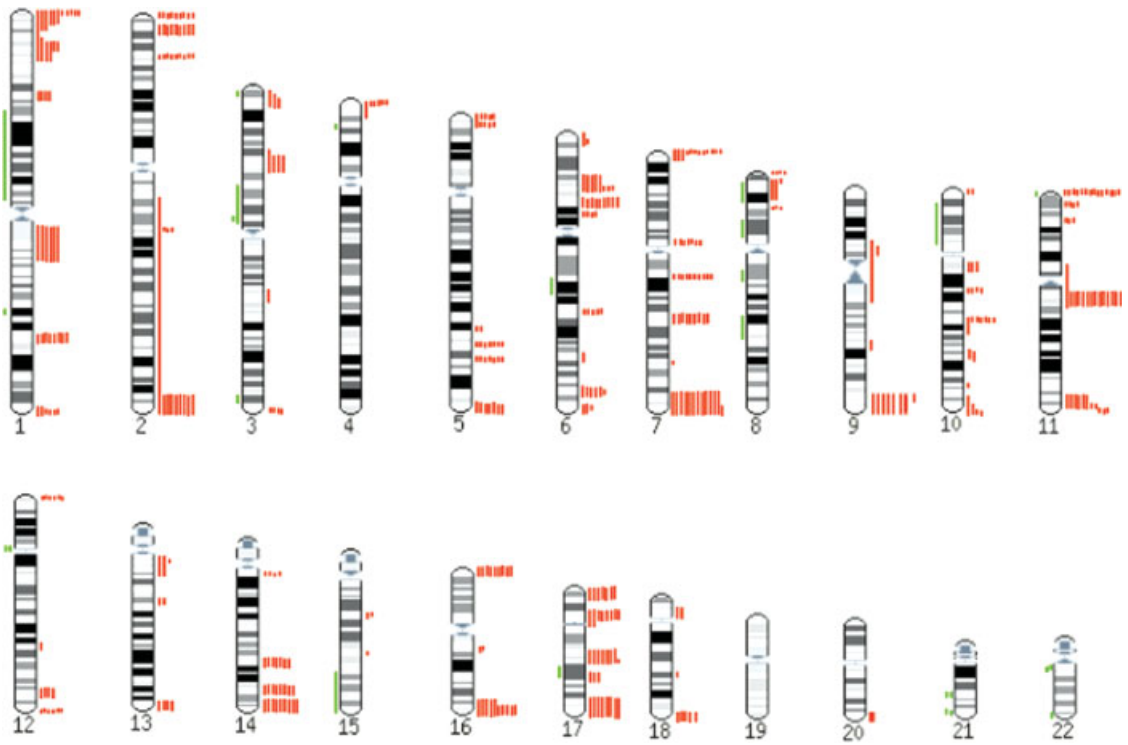

Figure 1. Karyoview of genomic imbalances present in all patients. Bars to the right of each chromosome represent genomic gains and bars to the left genomic losses. [Color figure can be viewed in the online issue, which is available at www.interscience.wiley.com.]

The nonparametric Mann-Whitney U-test was employed using Minitab version 13 to compare the significance of the different gene copy numbers of the tested target genes (Whitney, 1997).

Survival Statistics

Overall survival (OS) was estimated using the Kaplan–Meier method. Survival time was from the date of diagnosis to the date of death from any cause or the date of last contact if the patient is still alive. Cox regression analysis was used to estimate hazard ratios and 95% confidence intervals for the different groups of patients. *P* values below 0.05 indicate significant differences between groups of patients. Stata 10.0 software was used for this statistical analysis (StataCorp, College Station, TX).

RESULTS

Detection of Chromosomal Imbalances in Pediatric ALK-Positive ALCL

We have analyzed 18 samples (from 15 patients) of pediatric ALK-expressing ALCL by 1 MB aCGH for the presence of recurrent genomic gains and losses. Overall, genomic gains (range of 1–38/patient) were more prevalent than losses (range of 0–3/patient), with some regions showing both gains and losses in different patients (three patients) (Table 1). We did not detect any regions of high level genomic amplification. The chromosome displaying the highest number of gains was Chromosome 11 with 92.9% of patients ($n = 15$) demonstrating imbalances at 11p15.5, 11q13.1, and/or 11q12.3, 66.7% at 11q12.2 and/or 11q13.2-11q13.3 and/or 11q13.4 followed by Chromosome 7 with 66.7% of patients demonstrating gains at 7q36.3 (Fig. 1 and Table 1). The total number of genomic imbalances among the patient samples had a median value of 14 with a range of 2–40. Of the 13 patients with clinical data, 6 had 2–12 imbalances and the remaining 7 patients had 14–40 imbalances. Regions of loss were not associated with known tumor suppressors such as *RB1*, *TP53*, or *CDKN2A*; in fact the region encoding *TP53* (17p13.1) was gained in six cases. However, in 5/6 with gain of this region the negative regulator of TP53, MDM4 on 1q32.1 was also gained. In the same five cases, the genomic region encoding the retinoblastoma binding protein 5 (*RBBP5*) encoded on an adjacent BAC was also gained.

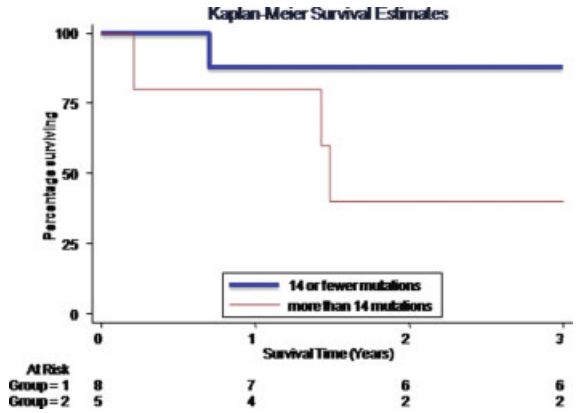

Figure 2. Kaplan–Meier survival curve demonstrating the poor prognosis for patients with greater than 14 genomic imbalances. [Color figure can be viewed in the online issue, which is available at www.interscience.wiley.com.]

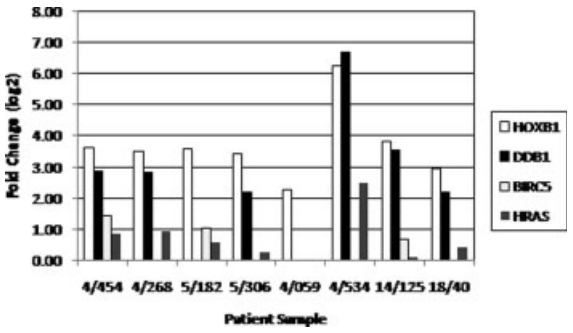

Figure 3. Q-PCR confirmation of genomic gains.

RBBP5 preferentially binds to underphosphorylated RB1 in the E2F binding pocket suggesting that E2F is free to transcribe genes required for S-phase progression.

Analysis of gene ontology demonstrated an over-representation of gene products involved in protein binding (23%) in the molecular function category, transcription (30%) in the biological function category and equal levels of membrane, cellular and nuclear localized proteins (15%) in the cellular localization category.

Relapse and Survival

Of the 13 EICNHL ALCL99 cases, samples were isolated from pediatric patients at first presentation (age range 3.1–16.6 years, median age of 12.7 years). Two patients could be analyzed both at presentation and relapse and, for one of these patients, at second relapse following presentation. Among the 13 patients with follow-up data overall survival was 68.4% at 3 years with only 1 death occurring after this time.

Interestingly, comparison of biopsy specimens taken at presentation and relapse from one patient (sample 4/268) demonstrated an increase in regions of genomic gain at relapse (sample 4/303) from 12 to 25. This patient died 8.5 months following initial diagnosis. An additional patient (sample 4/502) demonstrated one genomic gain and one loss at presentation, with a different loss and gain at first relapse (sample 4/503) but an increase to nine gains at second relapse (sample 4/534). This patient is still alive at 6.8 years following diagnosis. Indeed there was a trend toward increased survival at 3 years post diagnosis in patients with fewer than or equal to 14 ($n = 8$) copy number changes (87.5%, 95% CI = 38.7–98.1 vs. 40%, 95% CI = 5.2–75.3) (Fig. 2). The hazard ratio of 5.5 suggests that the mortality rates of patients with more than 14 copy number changes is five times higher than those with less than 14 (Fig. 2), although due to the small number of patients the confidence intervals vary widely (95% confidence interval = 0.57–53) and statistical significance was not reached ($P = 0.14$). These data require corroboration by a larger, independent study.

Q-PCR Confirmation of Genomic Gains

To confirm the genomic gains identified by aCGH we performed Q-PCR on a selected set of target genes. We chose to examine the status of *DDB1* on 11q12.2, *BIRC5* on 17q25.3, and *HOXB1* on 17q21.32. These genes were chosen because of their potential oncogenic effects. An increase in *HOXB1* gene copy number was seen by Q-PCR in all cases that demonstrated a gain in this genomic region by aCGH (Fig. 3, Supporting Information Table 2). In addition, some cases that did not demonstrate a gain by aCGH did by Q-PCR suggesting that more cases may carry gains of the HOXB genes than detectable by aCGH alone (Supporting Information Table 2). ALCLs displaying gains in the genomic region encoding the *HOXB1* cluster were not of any particular cell immunophenotype with equal numbers of null and T-cell phenotype. Likewise, gains in *DDB1* and *BIRC5* were observed confirming the aCGH data but again were not associated with any distinct disease phenotype.

Differential Association of HOXB1, DDB1, and BIRC5 Gains with Overall Survival at 5 Years

In our patient population ($n = 15$), 53.3% demonstrated gains of 17q21.32 (BAC RP11-125K7), a

TABLE 3. Survival Rates of Patients With and Without HOXB1, DDB1, and BIRC5 Gains

		N (patients)	Deaths	Survival at 3 years	95% CI
HOXB1 gain	Present	5	2	60	13–88
	Absent	8	2	75	22–93
DDB1 gain	Present	7	4	38	6–72
	Absent	6	0	100	–
BIRC5 gain	Present	3	2	33	1–77
	Absent	10	2	80	41–95

genomic region encoding the *HOXB* cluster alone. We focused on *HOXB1* for further study and demonstrated by Q-PCR that this region is increased by 2–6-fold (Fig. 3). Furthermore, statistical analysis revealed that the presence or absence of *HOXB* gains are not of prognostic significance (60% survival at 3 years with ($n = 5$) versus 75% survival without ($n = 8$) *HOXB* gain) (Table 3). However, of the patients demonstrating gains of 11q12.2 (BAC RP11-286N22) containing the *DDB1* gene, only 38% survived 3 years ($n = 7$) suggesting some adverse prognostic effect (Table 3). Likewise, in patients with gains of 17q25.3 (BAC RP11-141D1S) containing the *BIRC5* gene, only 33% ($n = 3$) survived whereas in those patients not showing a gain of this region, 80% were alive at 3 years ($n = 10$) (Table 3). Furthermore, of the two patients whose relapse samples were analyzed, the first patient (who died 8.5 months following diagnosis) showed a gain of the region encoding *DDB1* and *BIRC5* whereas the second patient (still alive at 6.8 years) did not have a gain in either *BIRC5* or *DDB1* genomic regions at presentation or first relapse but went on to develop a gain in the region encoding DDB1 alone at second relapse. Confidence intervals for these data are shown in Table 3.

DISCUSSION

Our results suggest that lower numbers of genomic imbalances may be associated with improved survival for pediatric patients with ALK-expressing ALCL. These data are in contrast to a previous study in which no prognostic effect of the copy number abnormalities could be discerned from a mixed population of adult and pediatric ALK^+ ALCL (Salaverria et al., 2008). It would be interesting to know whether such a prognostic association could be identified if the pediatric cases among the cohort studied by Salaverria et al., (2008) were considered separately. Furthermore, the differences in results could be explained by technical factors: while we used aCGH, Salaverria et al., (2008) used conventional CGH of a lower resolution.

Like the study performed by Salaverria et al., (2008) we detected no high level amplifications, mainly low level genomic gains and very few losses. Specifically, we also detected gains on 2q, 7p, 17p, and 17q but were unable to detect any of the previously reported genomic losses. These data are in keeping with previously published reports of low levels of genomic alterations in ALCL (Chou et al., 1996; Pittaluga et al., 1997; Rosenwald et al., 1999; Cools et al., 2002; Onciu et al., 2003; Liang et al., 2004) and suggest that high level amplifications are not a feature in the pathogenesis of this disease.

Analysis of our data revealed genomic gains of regions encoding proteins previously associated with the pathogenesis of ALCL. For example, gains at 11p15.5 where the *HRAS* gene is located were detected among 80% of our patient population ($n = 15$). We have previously demonstrated that NPM-ALK activity results in activation of the Ras-MAP Kinase pathway leading to cell survival (Turner et al., 2007). We have also detected gains of the region encoding *BIRC5* in 40% of our patients ($n = 15$). BIRC5, otherwise known as survivin, has previously been detected in cell lines engineered to express NPM-ALK and is associated with a poor prognosis (Schlette et al., 2004; Piva et al., 2006). Schlette et al., (2004) previously reported a 5-year failure-free survival of only 34% ($n = 28$) of their patient population when expressing this gene. We have similarly detected a 5-year overall survival rate of only 33% in patients showing a gain of *BIRC5* although this is based on a patient population of only three in our study. In contradiction, a study by Nasr et al., (2007) of a purely pediatric population of mostly ALK^+ ALCL could not demonstrate expression of survivin in their patient population. The higher overall event-free survival of their patient population (72%, $n = 40$) is consistent with the hypothesis that BIRC5 expression is associated with poor prognosis (Nasr et al., 2007). BIRC5 is a member of the inhibitor of apoptosis family and contributes to resistance to apoptosis of cancer cells. It localizes to mitotic spindles by interaction with tubulin during mitosis and is believed to be inhibited by TP53. As a result BIRC5 may be expressed as a result of TP53 inactivity. Indeed, we have shown that NPM-ALK inhibits the activity of TP53 (Cui et al., 2009).

We have also detected gains in genomic regions encoding genes not previously associated with the pathogenesis of ALCL, for example the *HOXB* cluster on 17q21.32. *HOXB* genes have been reported to play a role in normal hematopoiesis, specifically in expansion of the stem cell pool (Argiropoulos and Humphries, 2007). *HOXB* genes are also expressed in activated T-lymphocytes contributing to cellular proliferation (Care et al., 1994). This is in keeping with the presumed activated T-cell phenotype of ALK-expressing ALCL. While *HOXB* genetic gain has no prognostic significance it may be involved in the proliferative capacity of the tumor cells and hence may present a potential therapeutic target.

We have also detected gains in the genomic region encoding the DNA damage binding protein DDB1 in 60% of patients. *DDB1* is on 11q12.2 and gain of this gene has been confirmed by Q-PCR. Gain of *DDB1* may represent a poor prognostic factor as only 38% of patients survive 3 years when carrying a genomic gain in the region encoding this gene ($n = 7$). DDB1 is a DNA damage sensor that is lacking in patients with xeroderma pigmentosum complementation Group E. Gains of this gene may lead to upregulation of DNA repair activity, for example following therapy and could lead to drug resistance and disease progression consistent with a poor prognosis.

Of course we cannot rule out the involvement of other genes also expressed from the genomic region represented by individual BACs. For example RP11-286N22 includes dihydroxyacetone kinase (*DAK*), cytochrome B ascorbate dependent 3 (*CYBASCB*), transmembrane protein 138 (*TMEM138*), cleavage and polyadenylation specificity factor 7 (*CYPSF7*) and synaptotagmin 7 (*SYT7*) as well as *DDB1*. Likewise, RP11-141D1S includes transmembrane channel like protein 8 (*TMC8*), synaptogyrin 2 (*SYNGR-2*), thymidine kinase cytosolic (*TKI*) and probable formamylaridase (*AFMID*) as well as *BIRC5*, while RP11-361K8 only includes the *HOXB* cluster from B1 to B9. In addition, at a resolution of 1 MB the gained regions may be wholly underestimated and may involve many genes encoded on neighboring regions outside of the duplicated BACS. Higher resolution tiling path arrays would clarify this.

In conclusion, we show that those cases with greater than 14 genomic imbalances had a poorer prognosis with the overall survival of these patients dropping from 85 to 40% at 3 years. Additionally, patients with gains in genomic regions encoding either *BIRC5* or *DDB1* genes display decreased survival rates. We therefore suggest that these genetic abnormalities may represent poor prognostic markers for ALK-positive ALCL in children.

ACKNOWLEDGMENTS

This is a Children's Cancer and Leukemia Group (CCLG) United Kingdom study. We are grateful to all CCLG centers for providing us with material. We also acknowledge the Cambridge NIHR Biomedical Research Centre. We are also indebted to Prof. Ming-Qing Du and Dr Koichi Ichimura for many helpful discussions.

REFERENCES

Argiropoulos B, Humphries RK. 2007. Hox genes in hematopoiesis and leukemogenesis. Oncogene 26:6766–6776.

Bai RY, Dieter P, Peschel C, Morris SW, Duyster J. 1998. Nucleophosmin-anaplastic lymphoma kinase of large-cell anaplastic lymphoma is a constitutively active tyrosine kinase that utilizes phospholipase C-gamma to mediate its mitogenicity. Mol Cell Biol 18:6951–6961.

Bai RY, Ouyang T, Miething C, Morris SW, Peschel C, Duyster J. 2000. Nucleophosmin-anaplastic lymphoma kinase associated with anaplastic large-cell lymphoma activates the phosphatidylinositol 3-kinase/Akt antiapoptotic signaling pathway. Blood 96:4319–4327.

Brugieres L, Le Deley MC, Rosolen A, Williams D, Horibe K, Wrobel G, Mann G, Zsiros J, Uyttebroeck A, Marky I, Lamant L, Reiter A. 2009. Impact of the methotrexate administration dose on the need for intrathecal treatment in children and adolescents with anaplastic large-cell lymphoma: Results of a randomized trial of the EICNHL Group. J Clin Oncol 27:897–903.

Care A, Testa U, Bassani A, Tritarelli E, Montesoro E, Samoggia P, Cianetti L, Peschle C. 1994. Coordinate expression and proliferative role of HOXB genes in activated adult T lymphocytes. Mol Cell Biol 14:4872–4877.

Chanudet E, Ye H, Ferry J, Bacon CM, Adam P, Muller-Hermelink HK, Radford J, Pileri SA, Ichimura K, Collins VP, Hamoudi RA, Nicholson AG, Wotherspoon AC, Isaacson PG, Du MQ. 2009. A20 deletion is associated with copy number gain at the TNFA/B/C locus and occurs preferentially in translocation-negative MALT lymphoma of the ocular adnexa and salivary glands. J Pathol 217:420–430.

Chiarle R, Gong JZ, Guasparri I, Pesci A, Cai J, Liu J, Simmons WJ, Dhall G, Howes J, Piva R, Inghirami G. 2003. NPM-ALK transgenic mice spontaneously develop T-cell lymphomas and plasma cell tumors. Blood 101:1919–1927.

Chiarle R, Voena C, Ambrogio C, Piva R, Inghirami G. 2008. The anaplastic lymphoma kinase in the pathogenesis of cancer. Nat Rev Cancer 8:11–23.

Chou WC, Su IJ, Tien HF, Liang DC, Wang CH, Chang YC, Cheng AL. 1996. Clinicopathologic, cytogenetic, and molecular studies of 13 Chinese Patients with Ki-1 anaplastic large cell lymphoma. Special emphasis on the tumor response to 13-cis retinoic acid. Cancer 78:1805–1812.

Cools J, Wlodarska I, Somers R, Mentens N, Pedeutour F, Maes B, De Wolf-Peeters C, Pauwels P, Hagemeijer A, Marynen P. 2002. Identification of novel fusion partners of ALK, the anaplastic lymphoma kinase, in anaplastic large-cell lymphoma and inflammatory myofibroblastic tumor. Genes Chromosomes Cancer 34:354–362.

Cui YX, Kerby A, McDuff FK, Ye H, Turner SD. 2009. NPM-ALK inhibits the p53 tumor suppressor pathway in an MDM2 and JNK-dependent manner. Blood 113:5217–5227.

Fujimoto J, Shiota M, Iwahara T, Seki N, Satoh H, Mori S, Yamamoto T. 1996. Characterization of the transforming activity of p80, a hyperphosphorylated protein in a Ki-1 lymphoma cell line with chromosomal translocation t(2;5). Proc Natl Acad Sci USA 93:4181–4186.

Johnson NA, Hamoudi RA, Ichimura K, Liu L, Pearson DM, Collins VP, Du MQ. 2006. Application of array CGH on archival formalin-fixed paraffin-embedded tissues including small numbers of microdissected cells. Lab Invest 86:968–978.

Liang X, Meech SJ, Odom LF, Bitter MA, Ryder JW, Hunger SP, Lovell MA, Meltesen L, Wei Q, Williams SA, Hutchinson RN, McGavran L. 2004. Assessment of t(2;5)(p23;q35) translocation and variants in pediatric ALK+ anaplastic large cell lymphoma. Am J Clin Pathol 121:496–506.

McCabe MG, Ichimura K, Liu L, Plant K, Backlund LM, Pearson DM, Collins VP. 2006. High-resolution array-based comparative genomic hybridization of medulloblastomas and supratentorial primitive neuroectodermal tumors. J Neuropathol Exp Neurol 65:549–561.

Morris SW, Kirstein MN, Valentine MB, Dittmer KG, Shapiro DN, Saltman DL, Look AT. 1994. Fusion of a kinase gene, ALK, to a nucleolar protein gene, NPM, in non-Hodgkin's lymphoma. Science 263:1281–1284.

Nasr MR, Laver JH, Chang M, Hutchison RE. 2007. Expression of anaplastic lymphoma kinase, tyrosine-phosphorylated STAT3, and associated factors in pediatric anaplastic large cell lymphoma: A report from the children's oncology group. Am J Clin Pathol 127:770–778.

Onciu M, Behm FG, Raimondi SC, Moore S, Harwood EL, Pui CH, Sandlund JT. 2003. ALK-positive anaplastic large cell lymphoma with leukemic peripheral blood involvement is a clinicopathologic entity with an unfavorable prognosis. Report of three cases and review of the literature. Am J Clin Pathol 120:617–625.

Pittaluga S, Wlodarska I, Pulford K, Campo E, Morris SW, Van den Berghe H, De Wolf-Peeters C. 1997. The monoclonal antibody ALK1 identifies a distinct morphological subtype of anaplastic large cell lymphoma associated with 2p23/ALK rearrangements. Am J Pathol 151:343–351.

Piva R, Pellegrino E, Mattioli M, Agnelli L, Lombardi L, Boccalatte F, Costa G, Ruggeri BA, Cheng M, Chiarle R, Palestro G, Neri A, Inghirami G. 2006. Functional validation of the anaplastic lymphoma kinase signature identifies CEBPB and BCL2A1 as critical target genes. J Clin Invest 116:3171–3182.

Rosenwald A, Ott G, Pulford K, Katzenberger T, Kuhl J, Kalla J, Ott MM, Mason DY, Muller-Hermelink HK. 1999. t(1;2)(q21;p23) and t(2;3)(p23;q21): Two novel variant translocations of the t(2;5)(p23;q35) in anaplastic large cell lymphoma. Blood 94:362–364.

Salaverria I, Bea S, Lopez-Guillermo A, Lespinet V, Pinyol M, Burkhardt B, Lamant L, Zettl A, Horsman D, Gascoyne R, Ott G, Siebert R, Delsol G, Campo E. 2008. Genomic profiling reveals different genetic aberrations in systemic ALK-positive and ALK-negative anaplastic large cell lymphomas. Br J Haematol 140:516–526.

Schlette EJ, Medeiros LJ, Goy A, Lai R, Rassidakis GZ. 2004. Survivin expression predicts poorer prognosis in anaplastic large-cell lymphoma. J Clin Oncol 22:1682–1688.

Turner SD, Alexander DR. 2005. What have we learnt from mouse models of NPM-ALK-induced lymphomagenesis? Leukemia 19:1128–1134.

Turner SD, Alexander DR. 2006. Fusion tyrosine kinase mediated signalling pathways in the transformation of haematopoietic cells. Leukemia 20:572–582.

Turner SD, Tooze R, Maclennan K, Alexander DR. 2003. Vav-promoter regulated oncogenic fusion protein NPM-ALK in transgenic mice causes B-cell lymphomas with hyperactive Jun kinase. Oncogene 22:7750–7761.

Turner SD, Merz H, Yeung D, Alexander DR. 2006. CD2 promoter regulated nucleophosmin-anaplastic lymphoma kinase in transgenic mice causes B lymphoid malignancy. Anticancer Res 26:3275–3279.

Turner SD, Yeung D, Hadfield K, Cook SJ, Alexander DR. 2007. The NPM-ALK tyrosine kinase mimics TCR signalling pathways, inducing NFAT and AP-1 by RAS-dependent mechanisms. Cell Signal 19:740–747.

van Dongen JJ, Langerak AW, Bruggemann M, Evans PA, Hummel M, Lavender FL, Delabesse E, Davi F, Schuuring E, Garcia-Sanz R, van Krieken JH, Droese J, Gonzalez D, Bastard C, White HE, Spaargaren M, Gonzalez M, Parreira A, Smith JL, Morgan GJ, Kneba M, Macintyre EA. 2003. Design and standardization of PCR primers and protocols for detection of clonal immunoglobulin and T-cell receptor gene recombinations in suspect lymphoproliferations: Report of the BIOMED-2 concerted action BMH4-CT98–3936. Leukemia 17:2257–2317.

Whitney J. 1997. Testing for differences with the nonparametric Mann-Whitney U test. J Wound Ostomy Continence Nurs 24:12.

Zamo A, Chiarle R, Piva R, Howes J, Fan Y, Chilosi M, Levy DE, Inghirami G. 2002. Anaplastic lymphoma kinase (ALK) activates Stat3 and protects hematopoietic cells from cell death. Oncogene 21:1038–1047.

Zhang Q, Raghunath PN, Xue L, Majewski M, Carpentieri DF, Odum N, Morris S, Skorski T, Wasik MA. 2002. Multilevel dysregulation of STAT3 activation in anaplastic lymphoma kinase-positive T/null-cell lymphoma. J Immunol 168:466–474.